Received: 28 November 2016 | Revised: 22 March 2017 | Accepted: 5 April 2017

DOI: 10.1002/chir.22713

SPECIAL ISSUE ARTICLE

WILEY

Enantioselective cytotoxicity of ZnS:Mn quantum dots in A549 cells

V.A. Kuznetsova[1] | A.K. Visheratina[2] | A. Ryan[1] | I.V. Martynenko[2] | A. Loudon[1] | C.M. Maguire[3] | F. Purcell-Milton[1] | A.O. Orlova[2] | A.V. Baranov[2] | A.V. Fedorov[2] | A. Prina-Mello[3] | Y. Volkov[3] | Y.K. Gun'Ko[1,2]

[1] Chemistry School, Trinity College Dublin, Dublin, Ireland

[2] Optical Physics and Modern Natural Science, ITMO University, Saint Petersburg, Russia

[3] Clinical Medicine, School of Medicine, Trinity College Dublin, Dublin, Ireland

Correspondence
V.A. Kuznetsova, Chemistry School Trinity College Dublin College Green, Dublin 2, Dublin, Ireland.
Email: v.kuznetsova.a@gmail.com

Funding information
Irish Research Council; Science Foundation Ireland, Grant/Award Number: SFI 12/IA/1300; Ministry of Education and Science of the Russian Federation, Grant/Award Number: 14.B25.31.0002

Abstract

Chirality strongly influences many biological properties of materials, such as cell accumulation, enzymatic activity, and toxicity. In the past decade, it has been shown that quantum dots (QDs), fluorescent semiconductor nanoparticles with unique optical properties, can demonstrate optical activity due to chiral ligands bound on their surface. Optically active QDs could find potential applications in biomedical research, therapy, and diagnostics. Consequently, it is very important to investigate the interaction of QDs capped with chiral ligands with living cells. The aim of our study was to investigate the influence of the induced chirality of Mn-doped ZnS QDs on the viability of A549 cells. These QDs were stabilized with D- and L-cysteine using a ligand exchange technique. The optical properties of QDs were studied using UV–Vis, photoluminescence (PL), and circular dichroism (CD) spectroscopy. The cytotoxicity of QDs was investigated by high content screening analysis. It was found that QDs stabilized by opposite ligand enantiomers, had identical PL and UV–Vis spectra and mirror-imaged CD spectra, but displayed different cytotoxicity: QDs capped with D-cysteine had greater cytotoxicity than L-cysteine capped QDs.

KEYWORDS

chirality, cytotoxicity, enantioselectivity, Mn-doped ZnS quantum dots, semiconductor nanocrystals, zinc sulfide

1 | INTRODUCTION

A chiral molecule has two mirror-image forms, known as enantiomers, which are not superimposable in three dimensions. Enantiomers have identical physical properties,[1] and differ only in the direction in which they rotate the polarization vector of circular polarized light.[1] Therefore, an enantiomer can be either levorotatory (L) or dextrorotatory (D). This phenomenon of rotating polarized light is specifically known as optical activity and can be directly studied using circular dichroism (CD) spectroscopy.[2]

Chirality plays a crucial role in chemistry, pharmacology, biology, and medicine, as most of the organic molecules comprising living organisms are chiral, such as amino acids, carbohydrates, proteins, DNA, etc.[3] The area of chirality-related research in nanoscience is rapidly expanding, due to the numerous potential applications of optically active nanoparticles (NPs), such as catalysis and sensing.[4-24] Optical activity may be induced in colloidal NPs through the exchange of the original achiral ligands with chiral ligands, such as cysteine, penicillamine, etc. Ligand exchange allows the creation of hydrophilic biocompatible NPs with induced

optical activity.[8,14,24,25] It has been recently shown that NPs capped with opposite enantiomers of chiral ligands demonstrate different biological activity, including cytotoxicity within living cells.[26-28]

There is a wide variety of NPs that are very promising for a range of biomedical applications.[29] In particular, quantum dots (QDs) are of great interest. QDs are semiconductor NPs that possess unique optical properties, such as large absorption coefficients, high photoluminescence (PL) quantum yield (up to 100%),[30] and excellent photo- and chemical stability.[5,31,32]

However, the cytotoxicity of heavy-metal-containing QDs, which are typically made from toxic materials such as CdS, CdSe, or CdTe, is the main problem limiting their in vivo application.[31,33-35]

Heavy-metal-free QDs, based on a ZnS core doped with manganese ions (ZnS:Mn), are a unique and relatively new type of colloidal nanomaterials that possess a number of advantages in comparison with traditional Cd-based QDs.[36] First, ZnS:Mn QDs do not display heavy-metal-associated toxicity within living cells and organisms.[35,37-39] Second, the PL maximum of ZnS:Mn is located at 585 nm, at the spectral range in which tissue autofluorescence is negligible, meaning the QDs are ideal labels for bioimaging.[39,40] In addition, ZnS:Mn QDs can be excited by three-photon excitation using a 920 nm light source within the near-infrared window of biological tissue.[36]

To the best of our knowledge, the effect of induced chirality on the cytotoxicity of ZnS:Mn has not yet been investigated. Specifically, we studied the toxicity of ZnS:Mn QDs stabilized with cysteine (Cys) molecules on A549 cancer cells. It was found that D-Cys-capped QDs exhibit greater toxicity than L-Cys-capped QDs.

2 | MATERIALS AND METHODS

All chemical reagents including products for cell culturing were purchased from Sigma-Aldrich (St. Louis, MO). All reagents were analytical grade and used without further purification.

The ZnS:Mn QDs were synthesized according to Yu et al.[36] The ligand exchange was carried out using the previously reported method.[26]

2.1 | Equipment

UV–Vis spectroscopy was carried out using a Varian/Cary (Palo Alto, CA) 50 spectrophotometer. PL spectroscopy was performed using a Cary Eclipse spectrofluorometer. CD spectroscopy was carried out using a Jasco (Tokyo, Japan) J-810 CD spectrometer operating under a N2 flow of 5–8 L min − 1. The hydrodynamic diameter of QDs was collected by dynamic light scattering (DLS) using the Zetasizer Nano ZS system. Transmission electron microscopy (TEM) of QDs was performed using a FEI Titan electron microscope without aberration correction operating at a beam voltage of 300 kV. QDs solutions were diluted to 0.1 mg mL − 1 and allowed to dry at room temperature on lacey carbon-coated copper grids. A cell viability assay was carried out using Cytell Cell Imaging System (GE HealthCare, Milwaukee, WI).

2.2 | The investigation of the QDs aggregation in biological medium

The aggregation of QDs in biological medium was established using DLS. To stabilize QDs in biological medium, 0.3 mg mL^{-1} of bovine serum albumin (BSA) was added to the aqueous solutions of L- and D-cysteine stabilized QDs (L-Cys-QDs and D-Cys-QDs) at a concentration of 32 μM and incubated in darkness overnight at room temperature. The resulting L−/D-Cys-BSA-QDs and initial L−/D-Cys-QDs were added to Dulbecco's modified Eagle medium (DMEM) containing 10% fetal bovine serum (FBS) (additions of QDs were 10% of volume). Samples were incubated overnight at room temperature and then DLS spectra were recorded.

2.3 | Cell line and culture

The human lung-derived A549 cancer cell line was purchased from ATCC (American Tissue Culture Collection, Rockville, MD). A549 were grown in supplemented DMEM medium (Gibco/Invitrogen, La Jolla, CA) containing 4.5 g L^{-1} glucose, 10% FBS, and 5 mg L^{-1} gentamicin in the incubator at 37 °C supplied with 5% CO_2.

2.4 | Cell viability assessment by high content screening

For cytotoxicity assays, the A549 cells were seeded in 96-well plates in 100 μL supplement DMEM medium at 37 °C for 24 h. Cell density was 5×10^3 cells/well. L- and D-Cys-QDs were incubated overnight with 0.3 mg mL^{-1} of BSA. Then QDs mixed with DMEM containing 10% FBS were added to cells and incubated at 37 °C for 24 h. QDs concentration ranged from 4–32 μM, the volume of maximum addition was 10 μL per well (10% of medium volume). After fixation in formaldehyde 3.7% for 30 min the cellular nuclei were stained with Hoechst 33432 dye and a cell imaging and recording was carried out using Cytell Cell Imaging System (GE Healthcare, Buckinghamshire, UK). Cell viability was estimated by high content screening (HCS) analysis using the preinstalled GE Cell Viability BioApp 2-color protocol at 10x magnification. Ten random fields were imaged

across the entire well area of each QDs concentration exposure point. Exposures were repeated three times. Average cell viability was calculated comparing data from experimental samples and negative control. Positive control was 100 μM valinomycin as indicated.

3 | RESULTS AND DISCUSSION

3.1 | Optical properties of ZnS:Mn QDs

The oleylamine stabilized ZnS:Mn QDs (oleylamine-QDs) were prepared using the previously reported high-temperature metal–organic synthesis.[36] Representative TEM and high-resolution (HR) TEM images of oleylamine-QDs in chloroform are displayed in Figure 1A. The TEM image shows that the QDs had approximately spherical shape and were monodispersed. The HR TEM image, presented in the insert in Figure 1A, shows a high degree of QDs crystallinity. Figure 1B shows a size distribution diagram of oleylamine-QDs. The average size of QDs was determined to be ~5.3 ± 0.7 nm.

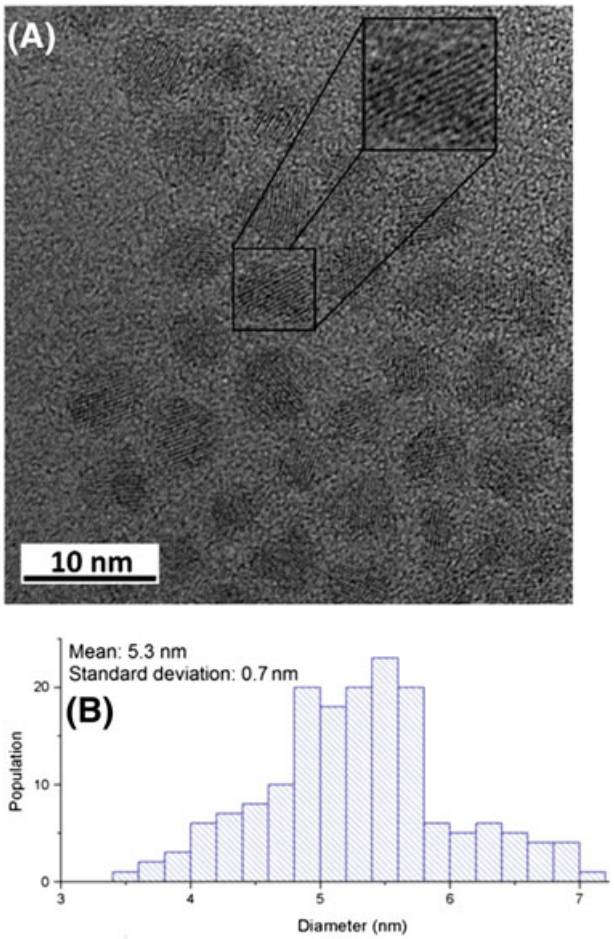

FIGURE 1 (A) TEM image and (B) size distribution diagram of oleylamine-stabilized ZnS:Mn QDs in chloroform. The insert in (a) shows HR TEM image of QDs

After the synthesis of the QDs, optical activity was induced by exchange of the original oleylamine ligands with D- and L-Cys ligands.[26] It has been demonstrated before that the ligand exchange method used in this work does not influence either the size or morphology of QDs.[41] Absorption and PL spectra of the QDs before and after the ligand exchange are presented in Figure 2. The edge of the first exciton absorption band was located at 300 nm approximately. The maximum of the QDs phosphorescence peak was located at 585 nm. The phosphorescence of ZnS:Mn QDs occurs as a result of energy transfer from the ZnS host to dopant Mn^{2+} ions.[36,42] The position of the QDs PL band maximum corresponded to that of Mn^{2+} ions.[36]

After the ligand exchange, the positions and shapes of the QDs absorption and PL bands remained unchanged. A comparative analysis of the fluorescent properties of the oleylamine-QDs and D−/L-Cys-QDs has shown that the PL quantum yield of QDs slightly decreased after the ligand exchange from 35% to 29%, but was identical for D−/L-Cys-QDs.

The CD spectra of L-Cys and D-Cys-QDs in aqueous solution are presented in Figure 2A. D- and L-Cys-QDs were optically active and exhibited pronounced opposite CD signals in the spectral regions of the QDs exciton absorption

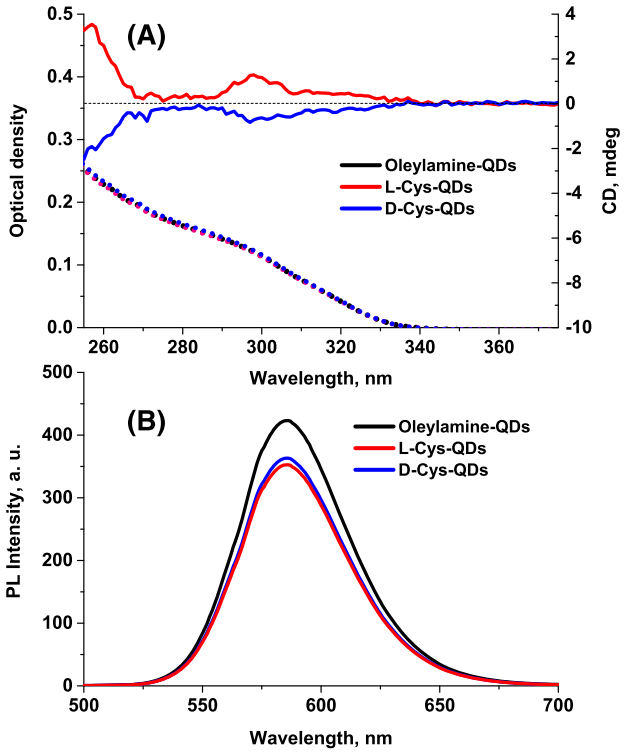

FIGURE 2 Optical properties of oleylamine-QDs before (in chloroform, black curve) and after ligand exchange with L- and DCys (in water, red and blue curves, respectively): (A) UV–vis and CD spectra, (B) PL spectra. QDs concentration was 3 μM in samples for CD measurements and 0.3 μM in samples for UV–vis and PL measurements

(255–340 nm) and chiral ligand absorption (255–270 nm). Oleylamine QDs in chloroform did not exhibit a CD signal (data not shown). Induction of optical activity in the spectral region of QDs exciton absorption after the ligand exchange can be attributed to hybridization of the QDs valence band states with the HOMO/LUMO orbitals of the chiral D- and L-Cys ligands.[25] The CD spectra of the D- and L-Cys-QDs provide evidence of successful oleylamine-to-cysteine ligand exchange and the formation of the enantiomeric D- and L-forms of optically active QDs.

3.2 | The investigation of QD aggregation in biological medium

It has been previously shown that cysteine stabilized QDs have a tendency to aggregate in biological media.[43] This phenomenon is explained by the fact that in media with high salt concentration, ions can interact with charged groups of Cys on the QDs surface and decrease QDs charge, allowing the NPs to come into close contact with each other and agglomerate. Adsorption of proteins on the NP surfaces may prevent aggregation of NPs and render them stable in biological media.[44]

Albumin is the most abundant protein in FBS, which is often used for cell culturing. In the present study we used BSA to prevent the aggregation of QDs in cell culture medium. For this purpose, QDs were incubated with BSA. Then L−/D-Cys-QDs and L−/D-Cys-BSA-QDs were added to medium (DMEM) containing 10% FBS. DLS spectra of QDs, presented in Figure 3, were recorded the next day to establish the aggregation of the QDs.

It is clearly seen that the D- and L-Cys-QDs without BSA formed clusters with an average hydrodynamic diameter of 70 ± 9 nm and 58 ± 11 nm, respectively, while the BSA-QDs remained monodispersed with an average hydrodynamic diameter of 7 ± 1 nm for both L- and D-Cys-QDs. Notably, BSA-QDs revealed PL QY of 29%, which is equal to L−/D-Cys-QDs PL QY. This indicates that the adsorption of BSA on ZnS:Mn QDs surface does not significantly change the PL QY of QDs. Further experiments on the QDs within living cells were carried out using L−/D-Cys-BSA-QDs.

3.3 | Cell viability assay

To compare the biological activity of L-Cys and D-Cys ZnS:Mn QDs, we studied their effect on A549 cell viability. It was anticipated that the cytotoxicity of the ZnS:Mn QDs would be significantly lower compared to that of cadmium-based QDs.[33-35,37-39] Nonetheless, ZnS-based QDs still exhibited cytotoxicity, which was dose-dependent. A wide range of NPs, even consisting of nontoxic elements, revealed nanocytotoxicity.[32,45,46]

As the size of a particle decreases, its surface area increases, as well as the ratio of structural defects per surface area. The defects can function as reactive sites, which can catalyze reactive oxygen species (ROS) generation. This could lead to oxidative stress and cell damage.[32] The presence of residual toxic organic ligands from the initial synthesis medium has also been associated with the cytotoxic nature of QDs.[31]

For the cytotoxicity analysis, A549 cells were incubated for 24 h with L−/D-Cys-BSA-QDs at a concentration ranging from 4–32 μM.

Cell viability was quantified by HCS analysis and the results are shown in Figure 4. It can been seen that viability level for A549 cells incubated with L−/D-Cys-BSA-QDs was higher than 80% in the range of the QDs concentration up to 16 μM. This is in agreement with literature data,[36,38] where toxicity of ZnS:Mn QDs also did not exceed 80% for the same cell line and range of QDs concentration. The

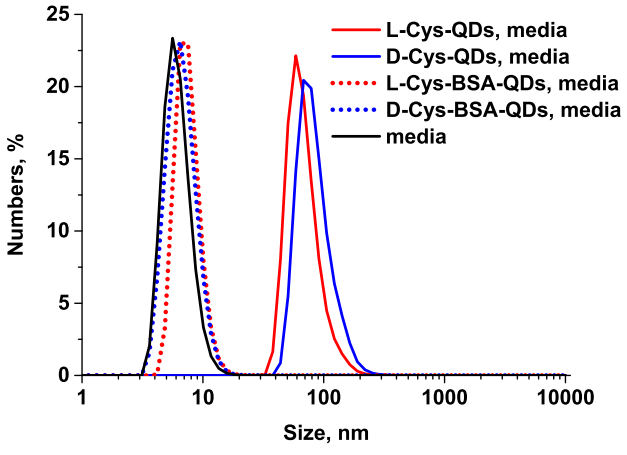

FIGURE 3 DLS spectra of L−/D-Cys-QDs and L−/D-Cys-BSA-QDs dispersed in biological medium (DMEM) containing 10% of FBS

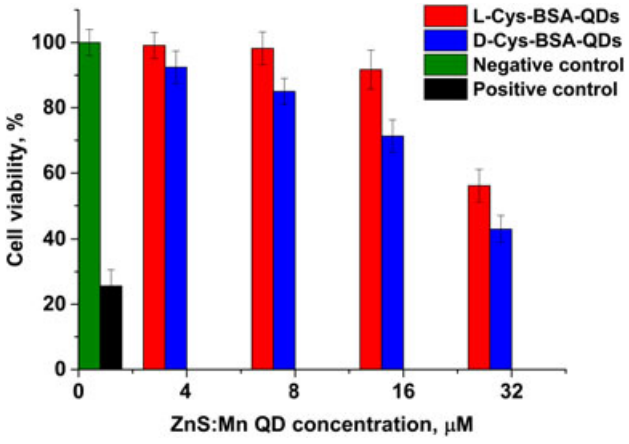

FIGURE 4 Histogram with cell viability data of A549 cells incubated with optically active QDs for 24 h at 37 °C. 100 μM Valinomycin was used for a positive control

toxicity of Cd-based QDs develops at ~0.1 μM, which is 2-fold higher.[34,38] For example, cell viability of A549 cells[38] and LNCaP cells[34] incubated with CdS and CdTe QDs, respectively, was about 50% and 60% at the QDs concentration of 0.1 μM.

Furthermore, between the two optically active forms investigated in this study, D-Cys-QDs showed higher cytotoxicity for the entire range of QDs concentrations (4–32 μM) compared to that of the L-Cys-QDs, with a maximum difference of ~20%. This result is in agreement with the work of Zhang et al.,[27] in which D-glutathione Au NCs were more toxic for GES-1 cells than L-glutathione Au NCs with a difference of ~40% at the maximum concentration.

Pure L- and D-Cys did not show cytotoxicity at the range of the concentrations used in our studies (up to 0.33 mg mL^{-1}). Similar data has also been reported by Zhang et al.[27] for pure L- and D-glutathione. This difference in cytotoxicity can be explained by the following effects. First, L-Cys and D-Cys-QDs can exhibit enantioselective cellular uptake.[26] This means that the concentration of QDs inside the cells and the corresponding cytotoxicity will be different. Second, L-Cys and D-Cys-QDs can induce different mechanisms of cytotoxicity, such as level of ROS generation, apoptosis, or autophagy.[27,28] Further investigation of the precise mechanism of different QDs cytotoxicity in living cells is a continuing area of interest for our research.

4 | CONCLUSION

In the present work we investigated the cytotoxic effects of optically active ZnS:Mn QDs in living A549 cells. We demonstrated that L-Cys and D-Cys-QDs had mirror-image CD spectra in the region of intrinsic QDs absorption and identical UV–Vis and PL spectra. However, most important, we found that the chirality of the ligands played a crucial role in the biological interaction with living cells. We found that the incubation with L-Cys-QDs resulted in a higher A549 cell viability than with D-Cys-QDs. Identification of this chirality-dependent cytotoxicity of QDs provides an important insight into the design of more biocompatible surface coatings. We believe that this could open new avenues for the further development of QDs for targeted biomedical imaging and other biological applications.

ACKNOWLEDGMENTS

The authors acknowledge the support of Irish Research Council, Science Foundation Ireland (grant SFI 12/IA/1300) and the Ministry of Education and Science of the Russian Federation for Grant 14.B25.31.0002.

REFERENCES

1. Clayden J, Greeves N, Warren S, Wothers P. *Organic Chemistry*. 1st ed. Oxford, UK: Oxford University Press; 2001:338. 1536 p.
2. Nina Berova P, Prasad L. *Nakanishi, Koji Woody, Robert W.* Comprehensive Chiroptical Spectroscopy. Hoboken, NJ: John Wiley & Sons; 2012.
3. Zhang M, Qing G, Sun T. Chiral biointerface materials. *Chem Soc Rev*. 2012;41(5):1972-1984.
4. Delgado-Pérez T, Bouchet LM, de la Guardia M, Galian RE, Pérez-Prieto J. Sensing chiral drugs by using CdSe/ZnS nanoparticles capped with N-acetyl-L-cysteine methyl ester. *Chem A Eur J*. 2013;19(33):11068-11076.
5. Medintz IL, Uyeda HT, Goldman ER, Mattoussi H. Quantum dot bioconjugates for imaging, labelling and sensing. *Nat Mater*. 2005;4(6):435-446.
6. Milton FP, Govan J, Mukhina MV, Gun'ko YK. The chiral nanoworld: Chiroptically active quantum nanostructures. *Nanoscale Horiz*. 2016;1(1):14-26.
7. Moloney MP, Gun'ko YK, Kelly JM. Chiral highly luminescent CdS quantum dots. *Chem Commun*. 2007;38:3900-3902.
8. Elliott SD, Moloney MP, Gun'ko YK. Chiral shells and achiral cores in CdS quantum dots. *Nano Lett*. 2008;8(8):2452-2457.
9. Govan JE, Jan E, Querejeta A, Kotov NA, Gun'ko YK. Chiral luminescent CdS nano-tetrapods. *Chem Commun*. 2010;46(33):6072-6074.
10. Gallagher SA, Moloney MP, Wojdyla M, Quinn SJ, Kelly JM, Gun'ko YK. Synthesis and spectroscopic studies of chiral CdSe quantum dots. *J Mater Chem*. 2010;20(38):8350-8355.
11. Gerard VA, Gun'ko YK, Defrancq E, Govorov AO. Plasmon-induced CD response of oligonucleotide-conjugated metal nanoparticles. *Chem Commun*. 2011;47(26):7383-7385.
12. Govorov AO, Gun'ko YK, Slocik JM, Gerard VA, Fan Z, Naik RR. Chiral nanoparticle assemblies: Circular dichroism, plasmonic interactions, and exciton effects. *J Mater Chem*. 2011;21(42):16806-16818.
13. Wojdyla M, Gallagher SA, Moloney MP, et al. Picosecond to millisecond transient absorption spectroscopy of broad-band emitting chiral CdSe quantum dots. *J Phys Chem C*. 2012;116(30):16226-16232.
14. Mukhina MV, Maslov VG, Baranov AV, et al. Intrinsic chirality of CdSe/ZnS quantum dots and quantum rods. *Nano Lett*. 2015;15(5):2844-2851.
15. Mukhina MV, Baimuratov AS, Rukhlenko ID, et al. Circular dichroism of electric-field-oriented CdSe/CdS quantum dots-in-rods. *ACS Nano*. 2016;10(9):8904-8909.
16. Wu XL, Xu LG, Ma W, et al. Propeller-like nanorod-upconversion nanoparticle assemblies with intense chiroptical activity and luminescence enhancement in aqueous phase. *Adv Mater*. 2016;28(28):5907-5915.
17. Kim Y, Yeom B, Arteaga O, et al. Reconfigurable chiroptical nanocomposites with chirality transfer from the macro- to the nanoscale. *Nat Mater*. 2016;15(4):461-468.

18. Zhou YL, Marson RL, van Anders G, et al. Biomimetic hierarchical assembly of helical supraparticles from chiral nanoparticles. *ACS Nano*. 2016;10(3):3248-3256.

19. Suzuki N, Wang YC, Elvati P, et al. Chiral graphene quantum dots. *ACS Nano*. 2016;10(2):1744-1755.

20. Zhang J, Feng WC, Zhang HX, et al. Multiscale deformations lead to high toughness and circularly polarized emission in helical nacre-like fibres. *Nat Commun*. 2016;7:10701-10709.

21. Li S, Xu LG, Ma W, et al. Dual-mode ultrasensitive quantification of micro RNA in living cells by chiroplasmonic nanopyramids self-assembled from gold and upconversion nanoparticles. *J Am Chem Soc*. 2016;138(1):306-312.

22. Yeom J, Yeom B, Chan H, et al. Chiral templating of self-assembling nanostructures by circularly polarized light. *Nat Mater*. 2015;14(1):66-72.

23. Hu T, Isaacoff BP, Bahng JH, et al. Self-organization of plasmonic and excitonic nanoparticles into resonant chiral supraparticle assemblies. *Nano Lett*. 2014;14(12):6799-6810.

24. Yeom B, Zhang H, Zhang H, et al. Chiral plasmonic nanostructures on achiral nanopillars. *Nano Lett*. 2013;13(11):5277-5283.

25. Tohgha U, Deol KK, Porter AG, et al. Ligand induced circular dichroism and circularly polarized luminescence in CdSe quantum dots. *ACS Nano*. 2013;7(12):11094-11102.

26. Martynenko IV, Kuznetsova VA, Litvinov IK, et al. Enantioselective cellular uptake of chiral semiconductor nanocrystals. *Nanotechnology*. 2016;27(7): 075102

27. Zhang C, Zhou Z, Zhi X, et al. Insights into the distinguishing stress-induced cytotoxicity of chiral gold nanoclusters and the relationship with GSTP1. *Theranostics*. 2015;5(2):134-149.

28. Li Y, Zhou Y, Wang HY, et al. Chirality of glutathione surface coating affects the cytotoxicity of quantum dots. *Angew Chem Int Ed*. 2011;50(26):5860-5864.

29. De M, Ghosh PS, Rotello VM. Applications of nanoparticles in biology. *Adv Mater*. 2008;20(22):4225-4241.

30. Linkov P, Krivenkov V, Nabiev I, Samokhvalov P. High quantum yield CdSe/ZnS/CdS/ZnS multishell quantum dots for biosensing and optoelectronic applications. *Mater Today Proc*. 2016;3(2): 104-108.

31. Resch-Genger U, Grabolle M, Cavaliere-Jaricot S, Nitschke R, Nann T. Quantum dots versus organic dyes as fluorescent labels. *Nat Methods*. 2008;5(9):763-775.

32. Volkov Y. Quantum dots in nanomedicine: Recent trends, advances and unresolved issues. *Biochem Biophys Res Commun*. 2015;468(3):419-427.

33. Chen N, He Y, Su Y, et al. The cytotoxicity of cadmium-based quantum dots. *Biomaterials*. 2012;33(5):1238-1244.

34. Su YY, Hu M, Fan CH, et al. The cytotoxicity of CdTe quantum dots and the relative contributions from released cadmium ions and nanoparticle properties. *Biomaterials*. 2010;31(18):4829-4834.

35. Li H, Li MY, Shih WY, Lelkes PI, Shih WH. Cytotoxicity tests of water soluble ZnS and CdS quantum dots. *J Nanosci Nanotechnol*. 2011;11(4):3543-3551.

36. Yu JH, Kwon SH, Petrasek Z, et al. High-resolution three-photon biomedical imaging using doped ZnS nanocrystals. *Nat Mater*. 2013;12(4):359-366.

37. Plumley JB, Akins BA, Alas GJ, et al. Non-cytotoxic Mn-doped ZnSe/ZnS quantum dots for biomedical applications. In: Parak WJ, Osinski M, Yamamoto KI, editors. Colloidal Nanoparticles for Biomedical Applications Ix. Vol. 8955, Proceedings of SPIE. Bellingham: Spie-Int Soc. Optical Engineering; 2014.

38. Manzoor K, Johny S, Thomas D, Setua S, Menon D, Nair S. Bioconjugated luminescent quantum dots of doped ZnS: A cytofriendly system for targeted cancer imaging. *Nanotechnology*. 2009;20(6):13

39. Geszke M, Murias M, Balan L, et al. Folic acid-conjugated core/shell ZnS:Mn/ZnS quantum dots as targeted probes for two photon fluorescence imaging of cancer cells. *Acta Biomater*. 2011;7(3):1327-1338.

40. Wu P, Yan XP. Doped quantum dots for chemo/biosensing and bioimaging. *Chem Soc Rev*. 2013;42(12):5489-5521.

41. Visheratina A, Purcell-Milton F, Serrano-García R, et al. Chiral recognition of optically active CoFe2O4 magnetic nanoparticles by CdSe/CdS quantum dots stabilized with chiral ligands. *J Mater Chem C*. 2017;5(7):1692-1698.

42. Fofanov YA, Pleshakov IV, Kuz'min YI. Laser polarization-optical detection of the magnetization process of a magnetically ordered crystal. *J Opt Technol*. 2013;80(1):64-67.

43. Conde J, Dias JT, Grazu V, Moros M, Baptista PV, de la Fuente JM. Revisiting 30 years of biofunctionalization and surface chemistry of inorganic nanoparticles for nanomedicine. *Front Chem*. 2014;2:48

44. Sperling RA, Parak WJ. Surface modification, functionalization and bioconjugation of colloidal inorganic nanoparticles. *Philos Trans A Math Phys Eng Sci*. 2010;368(1915):1333-1383.

45. Lewinski N, Colvin V, Drezek R. Cytotoxicity of nanoparticles. *Small*. 2008;4(1):26-49.

46. Nel A, Xia T, Madler L, Li N. Toxic potential of materials at the nanolevel. *Science*. 2006;311(5761):622-627.

How to cite this article: Kuznetsova VA, Visheratina AK, Ryan A, et al. Enantioselective cytotoxicity of ZnS:Mn quantum dots in A549 cells. *Chirality*. 2017;1-6. https://doi.org/10.1002/chir.22713